Bimolecular reaction of CH3 + CO in solid p-H2: Infrared absorption of acetyl radical (CH3CO) and CH3-CO complex

Prasanta Das and Yuan-Pern Lee

Citation: The Journal of Chemical Physics **140**, 244303 (2014); doi: 10.1063/1.4883519
View online: http://dx.doi.org/10.1063/1.4883519
View Table of Contents: http://scitation.aip.org/content/aip/journal/jcp/140/24?ver=pdfcov
Published by the AIP Publishing

Bimolecular reaction of CH_3 + CO in solid *p*-H_2: Infrared absorption of acetyl radical (CH_3CO) and CH_3-CO complex

Prasanta Das[1] and Yuan-Pern Lee[1,2,a)]
[1]*Department of Applied Chemistry and Institute of Molecular Science, National Chiao Tung University, Hsinchu 30010, Taiwan*
[2]*Institute of Atomic and Molecular Sciences, Academia Sinica, Taipei 10617, Taiwan*

(Received 17 April 2014; accepted 3 June 2014; published online 24 June 2014)

We have recorded infrared spectra of acetyl radical (CH_3CO) and CH_3-CO complex in solid *para*-hydrogen (*p*-H_2). Upon irradiation at 248 nm of $CH_3C(O)Cl$/*p*-H_2 matrices, CH_3CO was identified as the major product; characteristic intense IR absorption features at 2990.3 (ν_9), 2989.1 (ν_1), 2915.6 (ν_2), 1880.5 (ν_3), 1419.9 (ν_{10}), 1323.2 (ν_5), 836.6 (ν_7), and 468.1 (ν_8) cm^{-1} were observed. When $CD_3C(O)Cl$ was used, lines of CD_3CO at 2246.2 (ν_9), 2244.0 (ν_1), 1866.1 (ν_3), 1046.7 (ν_5), 1029.7 (ν_4), 1027.5 (ν_{10}), 889.1 (ν_6), and 723.8 (ν_7) cm^{-1} appeared. Previous studies characterized only three vibrational modes of CH_3CO and one mode of CD_3CO in solid Ar. In contrast, upon photolysis of a CH_3I/CO/*p*-H_2 matrix with light at 248 nm and subsequent annealing at 5.1 K before re-cooling to 3.2 K, the CH_3-CO complex was observed with characteristic IR features at 3165.7, 3164.5, 2150.1, 1397.6, 1396.4, and 613.0 cm^{-1}. The assignments are based on photolytic behavior, observed deuterium isotopic shifts, and a comparison of observed vibrational wavenumbers and relative IR intensities with those predicted with quantum-chemical calculations. This work clearly indicates that CH_3CO can be readily produced from photolysis of $CH_3C(O)Cl$ because of the diminished cage effect in solid *p*-H_2 but not from the reaction of CH_3 + CO because of the reaction barrier. Even though CH_3 has nascent kinetic energy greater than 87 kJ mol^{-1} and internal energy ~42 kJ mol^{-1} upon photodissociation of CH_3I at 248 nm, its energy was rapidly quenched so that it was unable to overcome the barrier height of ~27 kJ mol^{-1} for the formation of CH_3CO from the CH_3 + CO reaction; a barrierless channel for formation of a CH_3-CO complex was observed instead. This rapid quenching poses a limitation in production of free radicals via bimolecular reactions in *p*-H_2.
 [http://dx.doi.org/10.1063/1.4883519]

I. INTRODUCTION

The acetyl radical (also known as methyl carbonyl and ethanoyl, designated CH_3CO) is an important intermediate in the oxidation of hydrocarbons in the troposphere[1] and in combustion of biofuels.[2] It is also involved in the metabolism of acetaldehyde, $CH_3C(O)H$.[3] The CH_3CO radical might be formed in the atmosphere via several channels: the reactions of OH and Cl with $CH_3C(O)H$,[4–6] reaction of CH_3 with CO,[7,8] and UV photolysis of acetyl halides [$CH_3C(O)X$; X = F, Cl, Br, I] and methyl ketones such as $CH_3C(O)CH_3$, $CH_3C(O)CH_2CH_3$, and $CH_3C(O)C(O)CH_3$.[6,9,10]

Despite its importance, spectral investigations of CH_3CO are limited. Bennett and Mile prepared CH_3CO on depositing alternative layers of $CH_3C(O)Cl$ and Na atoms with various matrix hosts at 77 K and characterized the products with electron paramagnetic resonance (EPR).[11] Their analysis showed that CH_3CO is a $\sigma-$type radical with the unpaired electron located primarily on the carbon atom of the carbonyl moiety, but appreciable spin density was located on the adjacent carbon and oxygen atoms. The infrared (IR) spectrum of gaseous CH_3CO is unreported, and only three IR lines were reported for matrix-isolated CH_3CO despite numerous attempts. Shirk and Pimentel identified the IR absorption of CH_3CO, produced on reaction of $CH_3C(O)Cl$ with Li atoms in an Ar matrix;[12] two lines at 1844 and 1328 cm^{-1} were observed. Jacox deposited Ar and CH_3CO, produced from the gaseous reaction F + $CH_3C(O)H$ in which F atoms were generated in a microwave discharge, and reported three lines at 1875, 1420, and 1329 cm^{-1} for CH_3CO isolated in solid Ar.[13] Thompson *et al.* reported a weak feature of CH_3CO at 1875.3 cm^{-1} after a $CH_3C(O)H$/Ar matrix was bombarded with electrons.[14] Because of the matrix cage effect, it is difficult to prepare CH_3CO from photolysis *in situ* of precursors such as $CH_3C(O)Cl$ isolated in a matrix. Several workers reported that predominantly complexes of HCl and ketene were observed upon UV photolysis of $CH_3C(O)Cl$ in its amorphous or crystalline form,[15,16] or isolated in solid Ar or Xe.[16–18] Only in experiments when $CH_3C(O)Cl$ isolated in Xe was irradiated with laser light at 193 nm were two weak features at 1874 and 1320 cm^{-1} observed and assigned to CH_3CO; the authors proposed that under such conditions some Cl might escape from the original Xe cage.[18]

Acetyl chloride served as a convenient precursor of CH_3CO in the gaseous phase. Arunan reported that the C−C bond is stronger than the C−Cl bond in $CH_3C(O)Cl$ by 12 kJ mol^{-1} based on experimental enthalpies for the

a)Author to whom correspondence should be addressed. Electronic mail: yplee@mail.nctu.edu.tw.

formation of $CH_3C(O)Cl$, CH_3, ClCO, CH_3CO, and Cl.[19] Person *et al.* investigated the photodissociation dynamics of gaseous $CH_3C(O)Cl$ in a molecular-beam and observed a preferential fission of the C−Cl bond over the C−C bond at photolysis wavelength 248 nm.[20,21] The observed anisotropic angular distribution of Cl is characteristic of a prompt, impulsive dissociation of the C−C1 bond. The anisotropic angular distribution was observed also by Deshmukh *et al.* using photofragment ion-imaging.[22] These authors found also that a fraction of the primary photofragment CH_3CO subsequently decomposes to form CH_3 and CO. Shibata *et al.* employed the photofragment ion-imaging with a femtosecond laser to demonstrate that the dissociation of $CH_3C(O)Cl$ occurs within a period comparable to the laser pulse duration of 200 fs.[23] Using photofragment translation spectroscopy, North *et al.* investigated the photolysis dynamics of $CH_3C(O)Cl$ at 248 nm and reported that ∼35% of CH_3CO underwent secondary decomposition to form $CH_3 + CO$,[24] consistent with a quantum yield of 0.28 for CH_3 from CH_3CO reported by Desmukh and Hess.[25] North *et al.* also determined the barrier for decomposition of CH_3CO to be 71 ± 4 kJ mol^{-1};[24] this value was supported by Shibata *et al.*[26] In contrast, Tang *et al.* excited $CH_3C(O)Cl$ at 235 nm and employed velocity map imaging to determine the barrier height for dissociation of CH_3CO to $CH_3 + CO$ as 59 kJ mol^{-1}.[27] The enthalpy of formation (ΔH_f^0) for CH_3CO at 298 K was determined to be −(9.8 ± 1.8) kJ mol^{-1} with the threshold photoelectron-photoion coincidence technique.[28] Liu *et al.* photolyzed at 248 nm $CH_3C(O)Cl$ in the presence of Ar or O_2 and reported an additional dissociation channel leading to formation of HCl, CO, and CH_2; the latter two were proposed to result from the secondary decomposition of CH_2CO, the co-product of HCl.[29]

Several theoretical investigations of the decomposition of $CH_3C(O)Cl$ have been reported.[30–32] Chen and Fang employed the B3LYP and CAS(10,8) methods with cc-pVDZ and cc-pVTZ basis sets to optimize the geometries and the MR-CI method with CAS(10,8) wave functions to calculate the single-point energy to investigate the photodissociation of $CH_3C(O)Cl$. They reported a nearly barrierless path involving fission of C−Cl bond on the first excited-singlet (S_1) surface, resulting in fragmentation on a time scale of picosecond, followed by further decomposition of CH_3CO to CH_3 and CO.

In addition to photolysis of $CH_3C(O)Cl$, CH_3CO radical might be produced from the reaction $CH_3 + CO$. Watkins and Word performed the $CH_3 + CO$ reaction in the gaseous phase to generate chemically activated CH_3CO and analyzed the products with gas-liquid chromatograph.[7] They estimated an activation energy of 25.0 kJ mol^{-1} for this reaction and enthalpy of −17 kJ mol^{-1} for formation of CH_3CO from $CH_3 + CO$. Anastasi and Maw photolyzed azomethane in the presence of CO in the gaseous phase and monitored CH_3 and CH_3CO using molecular modulation;[33] they determined the activation energy of 27.6 kJ mol^{-1} for the reaction $CH_3 + CO \rightarrow CH_3CO$, in agreement with 27 kJ mol^{-1} predicted with the CCSD(T)/aug-cc-pVTZ method.[34] According to the calculations, the complex of CH_3 and CO, denoted CH_3-CO, is stabilized by ∼3 kJ mol^{-1} relative to $CH_3 + CO$, but no experimental observation of CH_3-CO has been reported. Hence, it would be interesting to record the IR spectrum of CH_3-CO and to compare it with that of CH_3CO.

Solid *para*-hydrogen (*p*-H_2) is known to have a diminished cage effect that allows the production of free radicals via photofragmentation *in situ* or photo-induced bimolecular reactions.[35–39] In this laboratory we took advantage of this unique property of *p*-H_2 to prepare free radicals from C−Cl bond fission of their Cl-containing precursors because the Cl fragment can escape from the original matrix cage upon photolysis. Examples include the photolysis of acryloyl chloride, $CH_2CHC(O)Cl$, to generate 3-propenonyl (•CH_2CHCO) radical[40] and the photolysis of methoxysulfinyl chloride, $CH_3OS(O)Cl$, to yield CH_3OSO.[41] We, thus, expect to produce CH_3CO from photolysis of $CH_3C(O)Cl$ isolated in *p*-H_2 to yield an IR spectrum of CH_3CO much improved from those in previous reports. We irradiated with UV light also a *p*-H_2 matrix containing CH_3I and SO_2 to produce five prominent IR features of CH_3SO upon annealing of the matrix to induce the $CH_3 + SO_2$ reaction.[42] The reaction of $CH_3 + CO$ is, hence, expected to be feasible in solid *p*-H_2 for the purpose of learning whether CH_3CO or CH_3-CO is formed.

We report here the observation of eight IR lines of CH_3CO upon photolysis of $CH_3C(O)Cl$. The corresponding features of CD_3CO were observed from photolysis of $CD_3C(O)Cl$ to confirm the assignments. In performing the reaction $CH_3 + CO$ in solid *p*-H_2, we observed IR features of CH_3-CO instead of CH_3CO, indicating that the barrier height to form CH_3CO prevents this reaction in solid *p*-H_2.

II. EXPERIMENTS

The matrix isolation system for IR absorption employed in this work is the same as previously described.[40,42,43] In brief, the gold-plated copper block, cooled to 3.2 K with a closed-cycle refrigerator system, serves as both a matrix sample substrate and a mirror to reflect the incident IR beam to the detector. For photodissociation experiments, a gaseous mixture of $CH_3C(O)Cl/p$-H_2, $CD_3C(O)Cl/p$-H_2, or $CH_3C(O)C(O)CH_3/p$-H_2 (1/2000−1/2500, flow rate ∼15 mmol h^{-1}) was deposited over a period of ∼9 h. For photo-induced bimolecular reactions, gaseous mixtures of CH_3I/p-H_2 (1/1000) and CO/p-H_2 (1/1000) were co-deposited over a period of 9 h with a flow rate of 7 mmol h^{-1} for each mixture. IR absorption spectra were recorded with a Fourier-transform infrared (FTIR) spectrometer equipped with a KBr beam splitter and a HgCdTe detector at 77 K to cover a spectral range 400−4100 cm^{-1}. The spectrum was typically recorded at a resolution of 0.25 cm^{-1} and averaged with 600 scans at each stage of the experiment. The IR beam was passed through a filter (2.4 ILP-50, Andover) to block light of wavenumber greater than 4100 cm^{-1} to avoid the reaction of Cl with vibrationally excited H_2.[44]

The primary photolysis light at 248 nm was generated from a KrF excimer laser. For photodissociation of $CH_3C(O)Cl/p$-H_2 and $CD_3C(O)Cl/p$-H_2, the matrices were irradiated for up to 120 min and 30 min, respectively, using an average pulse energy of 5−6 mJ at a repetition rate of 3 Hz. For the photo-induced reaction, $CH_3I/CO/p$-H_2

matrix was irradiated for 15 min using pulses of average energy 3−4 mJ at repetition rate of 3 Hz. For photolysis of $CH_3C(O)C(O)CH_3$/*p*-H_2 and secondary photolysis we employed light at 355 nm and 532 nm generated from the third and second harmonic of a pulsed Nd:YAG laser, respectively.

$CH_3C(O)Cl$ (98%, Fluka), $CD_3C(O)Cl$ (99%, Aldrich), $CH_3C(O)C(O)CH_3$ (99%, Acros), CH_3I (99%, Riedel-de Haën), and CO (99.999%, Specialty Gases of America) were used without further purification. We used catalytic conversion to prepare gaseous *p*-H_2. Normal H_2 (99.9999%, Scott Specialty Gases) was passed through a trap at 77 K and a copper cell filled with hydrous iron (III) oxide catalyst (Aldrich) that was cooled to 10−15 K with a closed-cycle refrigerator. The temperature for *p*-H_2 conversion was typically set at 13 K at which the concentration of *o*-H_2 was less than 100 ppm.

We derived mixing ratios of reactants and products according to the method described in Ref. 40. For CH_3CO, CH_3, and CH_2CO, the integrated absorbance of 2−3 lines and predicted IR intensities predicted with the B3PW91/aug-cc-pVTZ method were used, whereas for CO (Ref. 45) and HCl (Ref. 46), integration of a single line and the reported experimental absorption cross sections were used.

III. THEORETICAL CALCULATIONS

We employed the GAUSSIAN 09 program[47] to calculate the harmonic and anharmonic vibrational wavenumbers and IR intensities of $CH_3C(O)Cl$, CH_3CO, and CH_3-CO using the B3PW91 and B3LYP density functional theories[48,49] with the aug-cc-pVTZ and 6-311G(2d,2p) basis sets, respectively.[50,51] Analytic first derivatives were utilized to optimize geometry, and anharmonic vibrational wavenumbers were calculated analytically at each stationary point.

A. $CH_3C(O)Cl$

The geometry and vibrational wavenumbers of $CH_3C(O)Cl$ have been well characterized.[52] The structural parameters of $CH_3C(O)Cl$ optimized with the B3PW91/aug-cc-pVTZ method are compared with those measured previously with electron diffraction (listed parenthetically)[53] in Fig. 1(a). The harmonic and anharmonic vibrational wavenumbers and relative intensities predicted with the B3PW91/aug-cc-pVTZ method for the fundamental modes of all vibrations of $CH_3C(O)Cl$ and $CD_3C(O)Cl$ are listed in Table SI of the supplementary material.[54] The anharmonic (harmonic) vibrational wavenumbers of $CH_3C(O)Cl$ with IR intensities greater than 20 km mol^{-1} are 1836 (1893), 1351 (1381), 1092 (1114), 935 (962), 600 (606), and 435 (439) cm^{-1}. Those of $CD_3C(O)Cl$ are 1855 (1891), 1103 (1145), 948 (967), and 554 (560) cm^{-1}.

B. CH_3CO radical and other possible products

The geometry and vibrational wavenumbers of CH_3CO have been reported.[55–57] The structural parameters of CH_3CO optimized with the B3PW91/aug-cc-pVTZ method are shown

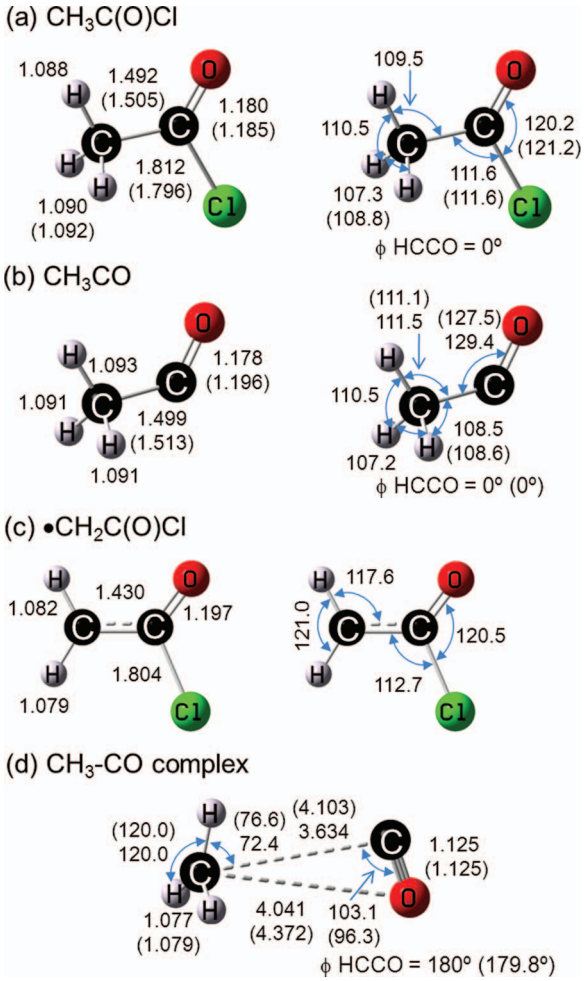

FIG. 1. Geometries of $CH_3C(O)Cl$ (a), CH_3CO (b), and $•CH_2C(O)Cl$ (c) predicted with the B3PW91/aug-cc-pVTZ method, and geometry of the CH_3-CO complex (d) predicted with the B3LYP/6-311G(2d,2p) method. Reported parameters obtained by gas-phase electron diffraction for (a)[53] and those predicted for (b) with the MP(full)/6-31G* method[57] and (d) with the B3PW91/6-311G(2d,2p) method are listed in parentheses. Bond distances are in Å and angles are in degrees.

in Fig. 1(b); those predicted with the MP(full)/6-31G* method[57] for CH_3CO are listed in parentheses for comparison. The harmonic and anharmonic vibrational wavenumbers and relative intensities predicted with the B3PW91/aug-cc-pVTZ method for the fundamental modes of all vibrations of CH_3CO and CD_3CO are listed in Table I. The anharmonic (harmonic) vibrational wavenumbers of CH_3CO with IR intensities greater than 10 km mol^{-1} are 1918 (1938), 1405 (1447), 1402 (1443), 1315 (1346), and 1039 (1049) cm^{-1}; corresponding values of CD_3CO are 1910 (1936), 1014 (1033), 1018 (1042), 1112 (1074), and 882 (904) cm^{-1}, respectively.

Possible products in our photofragmentation experiments of $CH_3C(O)Cl$ include ketene (CH_2CO), 2-chloro-2-oxo ethyl [also known as chloroformylmethyl, $•CH_2C(O)Cl$], and chloromethane (CH_3Cl). Infrared spectra of CH_2CO and CH_3Cl and their deuterated species have been reported.[17,58] We have calculated vibrational wavenumbers and IR intensities of CH_2CO, $•CH_2C(O)Cl$, and CH_3Cl and compared them with available experimental vibrational wavenumbers in

TABLE I. Comparison of observed wavenumbers (cm^{-1}) and relative IR intensities of CH_3CO and CD_3CO in solid *p*-H_2 with their harmonic and anharmonic vibrational wavenumbers and IR intensities calculated with the B3PW91/aug-cc-pVTZ method.

			CH_3CO				CD_3CO			
ν_i	Sym.	Mode[a]	Harmonic	Anharmonic	*p*-H_2	Ar	Harmonic	Anharmonic	*p*-H_2[c]	Isotopic ratio[b]
ν_1	A′	a-ν_{CH3}	3122 (4.9)[d]	2974	2989.1 (1.9)[d]		2313 (3.1)[d]	2230	2244.0 (3.4)[d]	0.751 (0.750)
ν_2	A′	s-ν_{CH3}	3026 (4.7)	2901	2915.6 (2.9)		2170 (1.5)	2152		
ν_3	A′	$\nu_{C=O}$	1938 (100)	1918	1880.5 (100)	1875	1936 (100)	1910	1866.1 (100)	0.992 (0.996)
ν_4	A′	δs-$_{CH2}$	1447 (14.2)	1405	1419.9 (8.0)[e]	1420	1033 (11.1)	1014	1029.7 (10.9)	0.725 (0.722)
ν_5	A′	u_{CH3}	1346 (9.6)	1315	1323.2 (10.9)	1329	1074 (4.7)	1112	1046.7 (3.5)	0.791 (0.845)[f]
ν_6	A′	δ_{CCH}	1049 (9.7)	1039	?		904 (7.9)	882	889.1 (9.3)	
ν_7	A′	ν_{C-C}	871 (2.8)	838	836.6 (4.5)		769 (0.1)	729	723.8 (<0.1)	0.865 (0.870)
ν_8	A′	δ_{CCO}	468 (3.3)	466	468.1?(2.8)		417 (2.2)	416		
ν_9	A″	a-ν_{CH2}	3128 (0.2)	2979	2990.3 (4.2)		2314 (0.2)	2237	2246.2 (sh)	0.751 (0.751)
ν_{10}	A″	a-δ_{CH3}	1443 (7.9)	1402	1419.9 (8.0)[e]		1042 (3.4)	1018	1027.5 (2.7)	0.724 (0.726)
ν_{11}	A″	oop-δ	948 (0.0)	896			747 (0.3)	718		
ν_{12}	A″	τ	112 (0.5)	100			93 (0.2)	82		
Reference			This work		This work	[13]	This work		This work	This work

[a]ν: stretch, δ: bend or deformation, δs: scissor, u: umbrella, τ: torsion, oop: out-of-plane, a:antisymmetric, and s: symmetric.
[b]Defined as the ratio of wavenumber of the isotopic species to that of natural species; theoretical values are listed in parentheses.
[c]Additional weak infrared feature observed at 2029.0, 1929.1, and 1914.2 cm^{-1} is tentatively assigned to $2\nu_4$ or $(\nu_4 + \nu_{10})$, $(\nu_5 + \nu_6)$, and $(\nu_4 + \nu_6)$, respectively.
[d]Percentage IR intensities relative to the most intense lines at 1918 and 1910 cm^{-1} for CH_3CO and CD_3CO with corresponding IR intensities 163.9 and 171.3 km mol^{-1}, respectively.
[e]Preferred assignment of this line is ν_{10}, but the possibility of ν_4 cannot be positively ruled out. See text for discussion.
[f]Isotopic ratio of calculated harmonic vibrational wavenumbers is 0.798. See text for discussion.

Table SII of supplementary material.[54] The corresponding values of the fully deuterated species are listed in Table SIII of supplementary material.[54]

The geometry of •$CH_2C(O)Cl$ optimized with the B3PW91/aug-cc-pVTZ method is presented in Fig. 1(c). The predicted anharmonic (harmonic) vibrational wavenumbers of •$CH_2C(O)Cl$ with IR intensities greater than 20 km mol^{-1} are 1682 (1718), 1416 (1444), 1136 (1157), 769 (774), and 602 (609) cm^{-1}.

C. CH_3-CO complex

The geometry of the CH_3-CO complex predicted with the B3LYP/6-311G (2d,2p) method is presented in Fig. 1(d); we were unable to obtain a stable optimized structure of CH_3-CO with the B3PW91/aug-cc-pVTZ method. The most stable structure of CH_3-CO is the *anti*-conformer in which O is *anti* to one C−H bond of CH_3. The distance between two C atoms is predicted with the B3LYP/6-311G (2d,2p) method to be 3.634 Å; this distance became 4.103 Å when the B3PW91/6-311G(2d,2p) method was used. At the B3LYP/6-311G (2d,2p) level of theory, the energy of the complex exceeded that of CH_3 + CO by 0.2 kJ mol^{-1}. A single-point energy calculation was performed on the B3LYP/6-311G (2d,2p) optimized structures with the CCSD/6-311G (2d,2p) method; the energy of CH_3-CO became −1.9 kJ mol^{-1} relative to CH_3 + CO.

The predicted anharmonic (harmonic) vibrational wavenumbers and IR intensities of CH_3, CO, and CH_3-CO are listed in Table II. Those of CH_3-CO with IR intensities greater than 5 km mol^{-1} are 3142 (3288), 2190 (2214), and 669 (517) cm^{-1}. The most intense line near 669 cm^{-1}

TABLE II. Comparison of observed wavenumbers (cm^{-1}) and relative IR intensities of CH_3 and the CH_3-CO complex in solid *p*-H_2 with their harmonic and anharmonic vibrational wavenumbers and IR intensities predicted with the B3LYP/6-311G(2d,2p) method.

	CH_3			CH_3-CO[b]		
ν_i [a]	Harmonic	Anharmonic	*p*-H_2	Harmonic	Anharmonic	*p*-H_2
ν_1	3290 (8.9)[c]	3155	3171.6/3170.6 (21.0)[c]	3291 (5.4)[c]	3144	3165.7 (sh)[c]
ν_2	3290 (8.9)	3140		3288 (6.5)	3142	3164.5 (15)
ν_3	3114 (0.0)	3002		3113 (0.0)	2995	
ν_4				2214 (86)	2190	2150.1 (67)
ν_5	1411 (3.7)	1385	1402.7/1402.4 (1.9)	1412 (2.7)	1380	1397.6 (1.0)
ν_6	1411 (3.7)	1386	1401.7 (2.6)	1410 (3.4)	1379	1396.4 (3.8)
ν_7	504 (100)	703	624.3/623.1 (100)	517 (100)	669	613.0 (100)
Ref.	This work		42	This work		This work

[a]The order of mode follows the predicted harmonic vibrational wavenumbers of the CH_3-CO complex.
[b]Additional modes are predicted to have harmonic (relative intensities)/anharmonic vibrational wavenumbers: 70 (0.1)/289, 63 (0.0)/0.1, 49 (0.0)/195, 25 (0.2)/168, and 20 (0.0)/−95 cm^{-1} for the CH_3-CO complex.
[c]Percentage IR intensities relative to the most intense line near 600 cm^{-1} are listed in parentheses. IR intensities of these lines of CH_3 and the CH_3-CO complex are predicted to be 69 and 81 km mol^{-1}, respectively.

corresponding to the C−H out-of-plane bending mode shows significant, likely overestimated, negative anharmonicity.

IV. EXPERIMENTAL RESULTS

A. Photolysis of $CH_3C(O)Cl/p\text{-}H_2$ matrices

The IR spectrum of a sample of $CH_3C(O)Cl/p\text{-}H_2$ (1/2500) deposited at 3.2 K for 9 h is shown in Fig. 2(a); observed lines are compared with values from gaseous experiments[59] and calculations in Table SI of supplementary material.[54] Our experimental observations are consistent with those reported for gaseous $CH_3C(O)Cl$. Lines at 1814.0, 1428.6, 1425.1, 1362.6, 1105.4, 952.0, and 603.9 cm^{-1} are more intense.

Gaseous $CH_3C(O)Cl$ at 298 K has UV absorption cross sections of $\sim 5.5 \times 10^{-20}$ cm^2 $molecule^{-1}$ at 248 nm and $\sim 2.5 \times 10^{-20}$ cm^2 $molecule^{-1}$ at 266 nm, respectively.[60] Light at these two wavelengths was initially tested for photolysis of $CH_3C(O)Cl$, but irradiation of the matrix sample with light at 248 nm produced lines of CH_3CO with intensities greater than after irradiation at 266 nm. Upon irradiation of the $CH_3C(O)Cl/p\text{-}H_2$ (1/2500) matrix at 248 nm for 2 h, lines of $CH_3C(O)Cl$ decreased in intensity and new features in several groups appeared. A difference spectrum obtained on subtracting the spectrum recorded upon deposition from that recorded after irradiation at 248 nm is presented in Fig. 2(b); lines pointing upwards indicate production and those pointing downward indicate destruction. Lines in group X at 2990.3, 2915.6, 2989.1, 1880.5, 1419.9, 1323.2, 836.6, and 468.1(?) cm^{-1} show similar behavior under varied conditions; the ? mark indicates an uncertain assignment because of a small intensity. The intensities of these lines decrease upon secondary photolysis at 532 nm, as shown in the difference spectrum of the matrix upon further irradiation at 532 nm, Fig. 2(c). These lines in group X are assigned to acetyl (CH_3CO) radical, to be discussed in Sec. V A.

As shown in Figs. 2(b) and 2(c), lines of ketene (CH_2CO) at 3064.5/3065.4, 2146.4/2147.6, 1383.0, 600.0, and 522.6 cm^{-1} also appeared upon photolysis at 248 nm but their intensities remained unchanged upon secondary photolysis at 532 nm; for the observed doublets, the more intense ones are listed first. The observed vibrational wavenumbers are similar to those reported in an Ar matrix[17] at 3053, 2138, 1378, 618, and 528 cm^{-1} and in the gaseous phase at 3069, 2151, 1388, 588, and 528 cm^{-1},[61] as compared in Table SII.[54] Weak lines at 2141.8 and 2140.7 cm^{-1}, marked CH_2CO' in Fig. 2(b), are tentatively assigned to a CH_2CO-HCl complex because a line at 2145 cm^{-1} was reported for this complex produced after photolysis at 266 nm of $CH_3C(O)Cl$ in solid Ar.[18] The line of HCl at 2894.3 cm^{-1} (Refs. 62 and 63) was observed upon photolysis at 248 nm; its intensity increased after further irradiation at 532 nm.

Weak lines of CH_3 at 3170.7, 1401.7, and 624.1 cm^{-1} appeared upon irradiation of the matrix at 248 nm;[42] their intensities increased significantly upon secondary photolysis at 532 nm, as shown in Fig. 2(c). Observed lines at 2146.0, 2143.0, 2140.6, and 2137.6 cm^{-1} are assigned to the rotational lines of CO according to the reports on CO isolated in $p\text{-}H_2$.[40,64,65]

The temporal evolution of the concentrations of these species as a function of photolysis period at 248 nm is shown in Fig. 3. We estimated the decrease in the mixing ratio of $CH_3C(O)Cl$ to be (13.6 ± 0.9) ppm and the increases in the mixing ratios of CH_3CO, CH_2CO, HCl, CH_3, and CO to be approximately (9.5 ± 1.7), (2.5 ± 0.2), (3.6 ± 0.7), (1.4 ± 0.3), and (0.5 ± 0.1) ppm upon photolysis of the matrix at 248 nm for 2 h. After secondary photolysis with light at 532 nm, the changes in the mixing ratios of CH_3CO, CH_3, and CO were estimated to be −(3.1 ± 0.8), (3.7 ± 0.2), and (2.6 ± 0.5) ppm, respectively.

An alternative precursor 2,3-butanedione, $CH_3C(O)C(O)CH_3$, was also employed to produce CH_3CO. The absorption spectrum of $CH_3C(O)C(O)CH_3/p\text{-}H_2$ (1/2500)

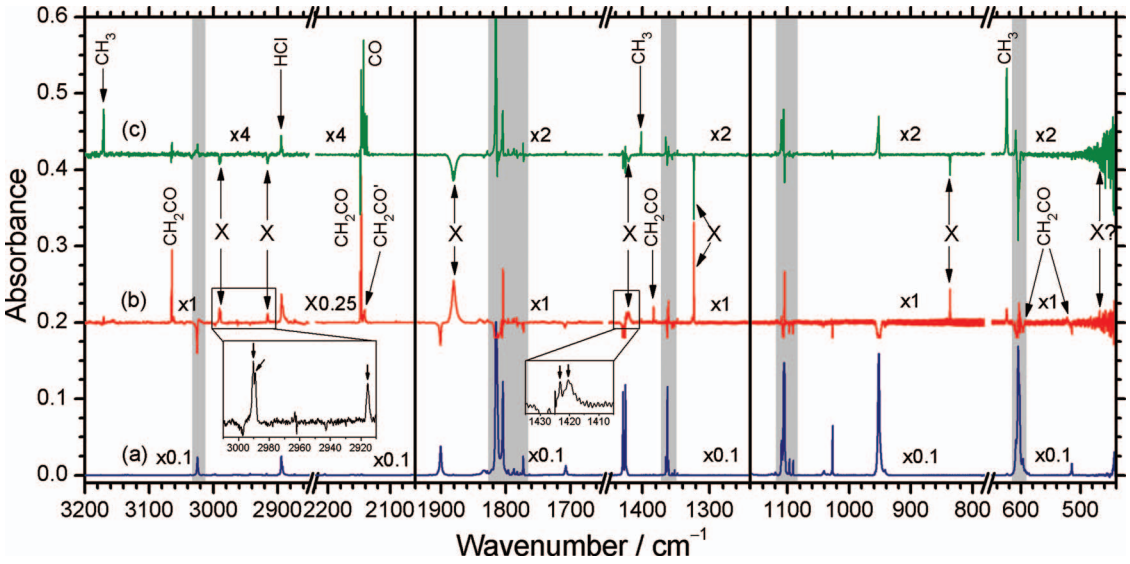

FIG. 2. (a) IR absorption spectrum of a $CH_3C(O)Cl/p\text{-}H_2$ (1/2500) matrix after deposition at 3.2 K for 9 h. (b) Difference spectrum of the matrix in (a) upon irradiation at 3.2 K with light at 248 nm for 2 h. (c) Difference spectrum obtained on further irradiation at 532 nm for 1 h. Lines in groups X, CH_2CO, CH_3, CO, and HCl are indicated. CH_2CO' indicates a complex of CH_2CO with HCl.

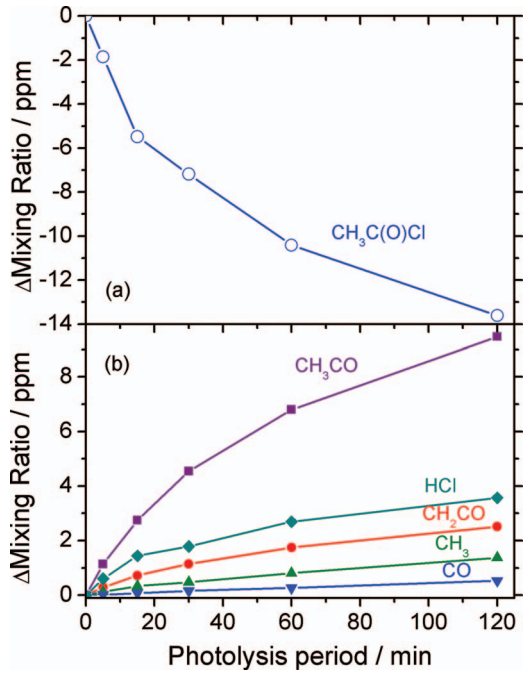

FIG. 3. Variations of mixing ratios as a function of period of photolysis at 248 nm for the precursor $CH_3C(O)Cl$ (a) and products CH_3CO, CH_2CO, HCl, CH_3, and CO (b). The initial concentration of $CH_3C(O)Cl$ was 214 ± 41 ppm.

matrix at 3.2 K deposited for 10 h is shown in Fig. S1(a) of the supplementary material.[54] Similar lines in group "X" were observed when this matrix was irradiated at 355 nm for 3 h, as shown in the difference spectrum in Fig. S1(b), but their intensities remained small even after irradiation prolonged to 6 h. This effect is likely due to secondary photolysis of CH_3CO at 355 nm. The difference spectrum obtained after photolysis of $CH_3C(O)Cl/p\text{-}H_2$(1/2500) at 248 nm is shown in Fig. S1(c) for comparison.

B. Photolysis of $CD_3C(O)Cl/p\text{-}H_2$ matrices

Similar experiments were performed with $CD_3C(O)Cl$ as a precursor. The IR spectrum of a sample of $CD_3C(O)Cl/p\text{-}H_2$ (1/2500) deposited at 3.2 K is shown in Fig. 4(a). Lines observed at 2273.2, 1817.1, 1129.0, 1039.8, 1034.7, 956.4, 873.4, 814.9, 558.8, 453.1, and 440.0 cm^{-1} are assigned to $CD_3C(O)Cl$, consistent with those reported for the gaseous phases,[59] as compared in Table SI of the supplementary material.[54] Figure 4(b) shows a difference spectrum of the matrix after irradiation at 248 nm for 30 min, indicating that the intensities of lines of $CD_3C(O)Cl$ decreased and new features in several groups appeared. Lines corresponding to group X (CH_3CO) that were observed in $CH_3C(O)Cl$ experiments shifted to 2244.0, 2246.2 (shoulder), 2029.0, 1929.1, 1914.2, 1866.1, 1046.7, 1029.7, 1027.5, 889.1, and 723.8 (not shown) cm^{-1}, marked as X_D in Fig. 4(b) and listed in Table I. The difference spectrum obtained after secondary photolysis at 532 nm is shown in Fig. 4(c); lines in group X_D decreased in intensity. We assigned these lines in group X_D to the CD_3CO radical, to be discussed in Sec. V B.

Lines of CH_2CO observed in $CH_3C(O)Cl/p\text{-}H_2$ experiments shifted to 2376.5, 2262.3/2262.2, 2116.2, 1226.2, and 849.9 cm^{-1}, as listed in Table SII;[54] they were readily assigned to CD_2CO according to values for CD_2CO in an Ar matrix.[17] The line of HCl at 2894.3 cm^{-1} shifted to 2092.6 cm^{-1}, identical to the value reported for DCl in $p\text{-}H_2$.[62] Lines of CH_3 observed at 3170.7 and 624.1 cm^{-1} shifted to 2383.9/2379.2 and 475.8/467.6 cm^{-1}, consistent with the reported values 2379 cm^{-1} for CD_3 in a $p\text{-}H_2$ matrix,[66] 2381, 1026, and 463 cm^{-1} in a Ne matrix,[67] and 453 and 465 cm^{-1} in an Ar matrix.[68] The lines of CH_3 at 1401.7 cm^{-1} are expected to shift to ~1034 cm^{-1}, but this region was severely interfered by absorption of $CD_3C(O)Cl$ near 1034 cm^{-1}. As expected, lines of CO did not shift. A weak line of ClCO observed at 1880.4 cm^{-1} is identical to that observed in $p\text{-}H_2$ upon photolysis of a $CH_2C{=}CHC(O)Cl/p\text{-}H_2$ matrix at

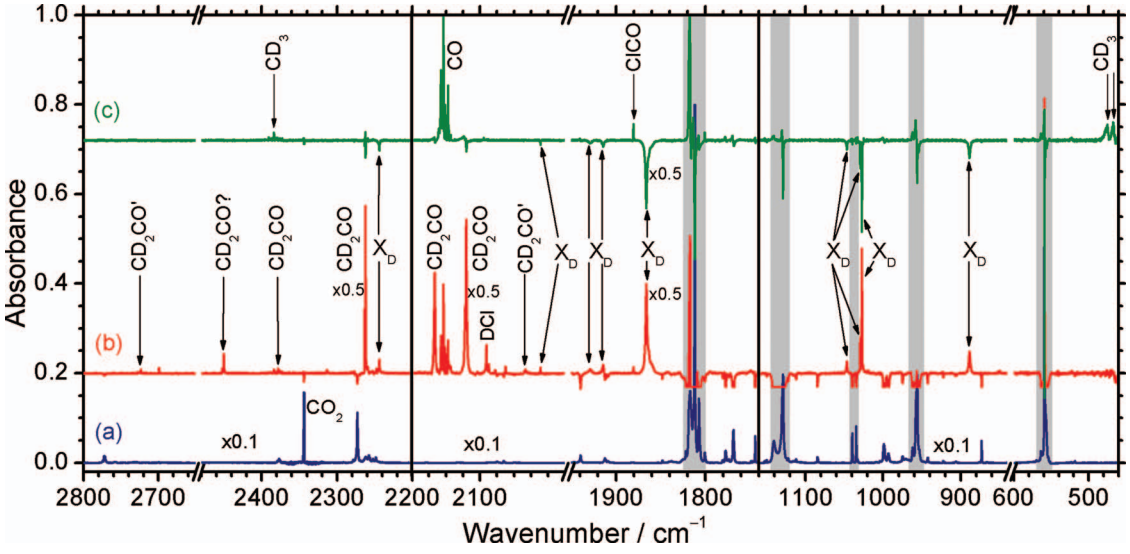

FIG. 4. (a) IR absorption spectrum of a $CD_3C(O)Cl/p\text{-}H_2$ (1/2500) matrix after deposition at 3.2 K for 9 h. (b) Difference spectrum of the matrix in (a) upon irradiation at 3.2 K with light at 248 nm for 30 min. (c) Difference spectrum obtained on further irradiation at 532 nm for 45 min. Lines in groups X_D, CD_2CO, CD_3, and CO are indicated; CD_2CO' indicates a complex of CD_2CO with DCl or HCl.

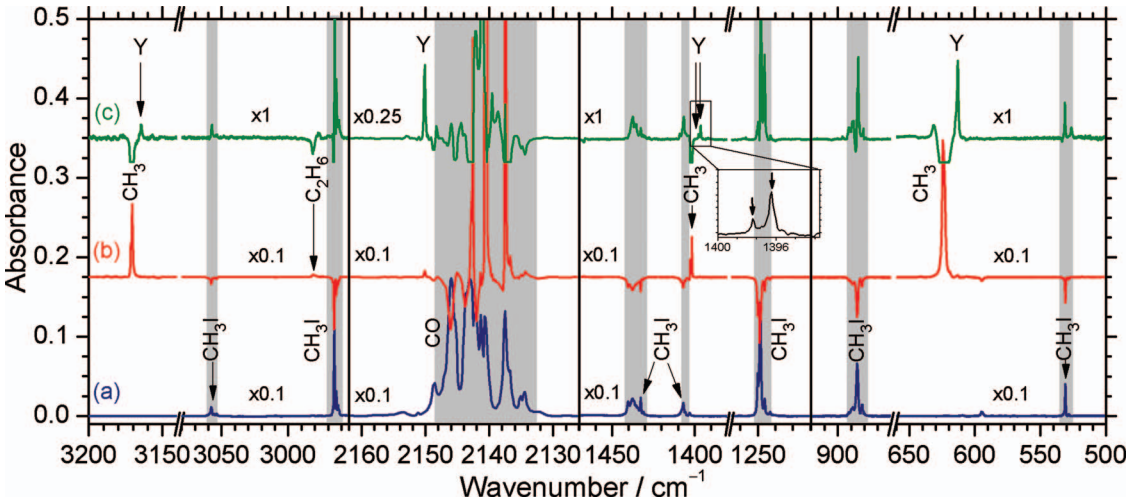

FIG. 5. (a) Partial IR spectra in regions of 500−660, 860−920, 1220−1265, 1380−1470, 2126−2162, 2955−3080, and 3140−3200 cm^{-1} of a $CH_3I/CO/p\text{-}H_2$ (1/1/2000) matrix after deposition at 3.2 K for 8 h. (b) Difference spectrum of the matrix in (a) upon irradiation at 3.2 K with light at 248 nm for 15 min. (c) Difference spectrum of the irradiated matrix after annealing at 5.1 K for 2 min and cooling to 3.2 K. Lines in groups Y, CH_3I, CH_3, C_2H_6, and CO are marked.

193 nm[40] and is consistent with the reported value of 1885 cm^{-1} in the gaseous phase.[69]

C. Photolysis of $CH_3I/CO/p\text{-}H_2$ matrices

We undertook blank tests with CO and CH_3I isolated in $p\text{-}H_2$ separately. The IR spectrum of a sample of $CO/p\text{-}H_2$ (1/4000) at 3.2 K exhibits intense vibration-rotational lines at 2146.0, 2143.0, 2140.6, and 2137.6 cm^{-1}.[40] The IR spectrum of a sample of $CH_3I/p\text{-}H_2$ (1/2000) at 3.2 K exhibits intense lines at 2965.1(ν_1), 1248.4 (ν_2), and 884.5 (ν_6) and weaker lines at 3057.5 (ν_4), 1432.5 (ν_5), and 531.3 (ν_3) cm^{-1}. Annealing of these matrices at 4.8 K for 5 min produced no observable change in the spectrum.

Gaseous CH_3I at 300 K has an absorption cross section of $\sim 1.0 \times 10^{-18}$ cm^2 molecule^{-1} near 254 nm.[70] We employed light at 248 nm from a KrF excimer laser to irradiate the matrix with the expectation that only CH_3I, but not CO, would be photolyzed so that reactions among only CH_3, CO, and I might occur. Irradiation of a $CH_3I/p\text{-}H_2$ (1/2000) matrix at 248 nm for 15 min yielded four sets of new lines at 3171.6/3170.6, 2780.1/2779.3, 1402.7/1402.4/1401.7, and 624.3/623.1 cm^{-1}. These lines are assigned to ν_3, $2\nu_4$, ν_4, and ν_2 modes of CH_3 in $p\text{-}H_2$.[42] Weak lines of C_2H_6 at 2981.9, 1467.5, and 821.3 (?) cm^{-1} were also observed, indicating that some CH_3 diffused and reacted with CH_3 to form C_2H_6.

The IR spectrum of a sample of $CH_3I/CO/p\text{-}H_2$ (1/1/2000) deposited at 3.2 K for 8 h is shown in Fig. 5(a). We observed lines of CH_3I and CO, but no additional feature assignable to the CH_3I-CO complex even after retaining the matrix overnight or annealing at 4.5 K for 10 min. Figure 5(b) represents the difference spectrum recorded after irradiation of the $CH_3I/CO/p\text{-}H_2$ (1/1/2000) matrix at 3.2 K with laser light at 248 nm for 15 min; the intensities of lines due to CH_3I decreased, the features due to CO show a first-derivative shape, and lines of CH_3 appeared. The first-derivative shape for lines of CO in the difference spectrum indicates that lines of CO might have shifted slightly upon irradiation. Extremely weak features at 2150.1 and 613.0 cm^{-1} were also observed; their intensities increased after annealing. Upon subsequent annealing at 5.1 K for 2 min, the intensities of lines due to CH_3 and CO decreased, those of CH_3I increased, and a group of new lines appeared at 3165.7, 3164.5, 2150.1, 1397.6, 1396.4, and 613.0 cm^{-1}, indicated as "Y" in Fig. 5(c). These features in group Y are assigned to the CH_3-CO complex, to be discussed in Sec. V C.

V. DISCUSSION

A. Assignment of lines in group X to the acetyl (CH_3CO) radical

Butler and co-workers observed that C−Cl bond fission was the major channel upon photolysis of gaseous $CH_3C(O)Cl$ at 248 nm.[20,21] Some CH_3CO fragments, thus, formed contained sufficient internal energy to enable further dissociation to CH_3 + CO; 28−35% of CH_3CO radicals decomposed.[24,25] Hence, CH_3CO, Cl, CH_3, and CO are the major products in this system.

Lines of group X were observed in UV photolysis of both $CH_3C(O)Cl$ and $CH_3C(O)C(O)CH_3$. The more intense lines in group X at 1880.5, 1419.9, and 1323.2 cm^{-1} have wavenumbers similar to values 1875, 1420, and 1329 cm^{-1} reported for CH_3CO isolated in solid Ar.[13] They are also near the anharmonic vibrational wavenumbers of 1918, 1405, and 1315 cm^{-1} for the C=O stretching (ν_3), CH_2 scissor (ν_4), and CH_3 umbrella (ν_5) modes of CH_3CO predicted with the B3PW91/aug-cc-pVTZ method. These observed lines in group X are, hence, likely due to CH_3CO. Because of the superior signal-to-noise (S/N) ratio, we were able to identify additional lines at 2990.3, 2989.1, 2915.6, 836.6, and, tentatively, 468.1 cm^{-1} that were previously unreported. These values are near quantum-chemically predicted values of 2979 (ν_9, CH_2 antisymmetric stretch), 2974 (ν_1, CH_3 antisymmetric stretch), 2901 (ν_2, CH_3 symmetric stretch), 838 (ν_7, C−C stretch), and 466 (ν_8, CCO bend) cm^{-1} for CH_3CO, as compared in Table I. The IR intensities of these lines were

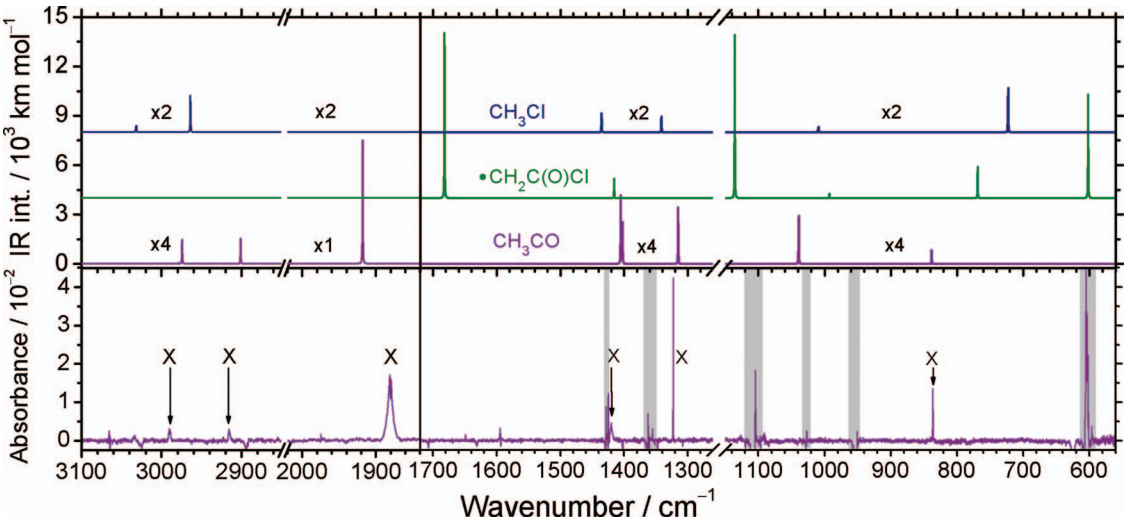

FIG. 6. Comparison of experimental spectrum with those simulated for possible candidates. (a) Inverted spectrum of Fig. 2(c), obtained upon secondary photolysis of the UV-irradiated matrix of $CH_3C(O)Cl/p\text{-}H_2$ with light at 532 nm for 1 h. IR spectra of CH_3CO (b), •$CH_2C(O)Cl$ (c), and CH_3Cl (d) were simulated according to anharmonic vibrational wavenumbers and IR intensities predicted with the B3PW91/aug-cc-pVTZ method. Regions of interference due to absorption of $CH_3C(O)Cl$ and CO are marked grey.

predicted to be less than 15% of the most intense line at 1880.5 cm^{-1}.

We inverted the difference spectrum in Fig. 2(c) and present it in Fig. 6(a) to compare with spectra of CH_3CO, •$CH_2C(O)Cl$, and CH_3Cl in Figs. 6(b)–6(d) simulated according to anharmonic vibrational wavenumbers and IR intensities predicted with quantum-chemical calculations. The observed lines in group X agree satisfactorily with the simulated spectrum of CH_3CO in terms of vibrational wavenumbers and IR intensities, but do not match with those predicted for •$CH_2C(O)Cl$ or CH_3Cl; the reported experimental values for CH_3Cl (Ref. 58) are near their predicted anharmonic vibrational wavenumbers, as listed in Table SII.[54]

After considering the photolytic behavior observed upon primary and secondary photolysis of the $CH_3C(O)Cl/p\text{-}H_2$ and $CH_3C(O)C(O)CH_3/p\text{-}H_2$ matrices and the agreement between predicted and observed vibrational wavenumbers and relative IR intensities, we assigned these features in group X to the IR absorption of acetyl (CH_3CO) radical. The most intense line at 1880.5 cm^{-1} corresponds to the C=O stretching mode. This value is near a value of 1875 cm^{-1} reported by Jacox,[13] but much greater than the value of 1844 cm^{-1} reported by Shirk and Pimentel;[12] the latter line might be perturbed by nearby Li atoms. The ν_1 (CH_3 antisymmetric stretching) and ν_9 (CH_2 antisymmetric stretching) modes were predicted at 2974 and 2979 cm^{-1} with IR intensities 4.9 and 0.2 km mol^{-1}, respectively. We observed a line at 2990.3 cm^{-1} and a shoulder at 2989.1 cm^{-1}, which we tentatively assigned to ν_1 and ν_9, respectively, according to observed relative IR intensities. The ν_4 (CH_2 scissor) and ν_{10} (CH_3 deformation) modes were predicted to be 1405 and 1402 cm^{-1} with IR intensities 14.2 and 7.9 km mol^{-1}, respectively, but only one line at 1419.9 cm^{-1} was observed in this region. The intense absorption of $CH_3C(O)Cl$ at 1425.1 and 1428.6 cm^{-1} and that of $CH_3C(O)C(O)CH_3$ at 1422.7 cm^{-1} might have interfered with the observation of the second line. We are, hence, unsure whether the assignment of the line at 1419.9 cm^{-1} should be ν_4 or ν_{10}. However, according to the observed relative IR intensity and relative position of ν_4 or ν_{10}, we prefer to assign this line at 1419.9 cm^{-1} to ν_{10} and the line for ν_4 might be interfered by absorption of $CH_3C(O)Cl$ and $CH_3C(O)C(O)CH_3$. The CCH bending (ν_6) mode was predicted to be 1039 cm^{-1} with IR intensity of 9.7 km mol^{-1}, but we observed no line in this region assignable to this mode. The reason for this absent line is unclear, but less likely to be due to interference of parent absorption, because we observed this mode in experiments on neither $CH_3C(O)Cl$ nor $CH_3C(O)C(O)CH_3$, which has distinct parent absorption lines in this region. The average deviation between observed wavenumbers and predicted anharmonic vibrational wavenumbers for CH_3CO is (14 ± 10) cm^{-1} with the largest deviation of ∼37 cm^{-1} for the ν_3 mode at 1880.5 cm^{-1}.

B. Assignment of lines in group X_D to the perdeuterated acetyl (CD_3CO) radical

The deuterium-substitution experiments provide additional support for the assignment of lines in group X to the acetyl radical. We show in Fig. S2(a) the inverted difference spectrum of the $CD_3C(O)Cl/p\text{-}H_2$ matrix after secondary photolysis with light at 532 nm [Fig. 4(c)]; the matrix was initially irradiated with light at 248 nm for 30 min before this step. The spectrum is compared with the IR spectra of CD_3CO, •$CD_2C(O)Cl$, and CD_3Cl, presented in traces (b)−(d) of Fig. S2, simulated according to predicted anharmonic vibrational wavenumbers and IR intensities. The agreement between the observed spectrum and the simulated spectrum of CD_3CO further supports our assignments of lines in group X (X_D) to CH_3CO (CD_3CO).

In Table I we compare the vibrational wavenumbers of lines in group X_D with the harmonic and anharmonic vibrational wavenumbers of CD_3CO calculated quantum-chemically. The assignments were made according to

predicted wavenumbers and IR intensities without ambiguity. A line of ν_2 predicted near 2152 cm^{-1} was unobserved because of interference from absorption of CO. The missing line of ν_6 in CH_3CO appeared at 889.1 cm^{-1}. The calculated isotopic ratios, defined as the ratio of vibrational wavenumbers of deuterated species to that of the natural species, are within 0.5% of observed values except for ν_5 for which observed ratio of 0.791 is much smaller than the predicted value of 0.845. The reason is that the predicted anharmonicity for this mode of CD_3CO is negative but that for CH_3CO is positive. If we use the harmonic vibrational wavenumbers, the predicted isotopic ratio of 0.798 becomes much nearer the experimental value.

Jacox observed a line at 1855 cm^{-1} in the D-substituted experiments and tentatively assigned it to CD_3CO.[13] We observed a characteristically intense line in group X_D at 1866.2 cm^{-1}. Considering the observed redshift of 6 cm^{-1} for CH_3CO from *p*-H_2 to Ar matrices, the redshift of 11 cm^{-1} for CD_3CO is slightly large, but not unacceptable. This line near 1855 cm^{-1} was the only one reported for CD_3CO; we observed seven additional lines in this experiment.

Three weak lines observed at 2029.0, 1929.1, and 1914.2 cm^{-1} in group X_D correspond to no predicted fundamental vibrational wavenumber of CD_3CO. The line observed at 2029.0 cm^{-1} might be tentatively assigned to the first overtone of ν_4 (fundamental mode at 1029.7 cm^{-1}) or a combination band of $(\nu_4 + \nu_{10})$, whereas lines at 1929.1 and 1914.2 cm^{-1} might be assigned to the combination bands of $(\nu_5 + \nu_6)$ and $(\nu_4 + \nu_6)$, respectively.

C. Assignment of lines in group Y to the CH_3-CO complex

As discussed previously, reactions among CH_3, CO, and I might occur upon UV photolysis of a CH_3I/CO/*p*-H_2 matrix at 248 nm; possible new products are CH_3CO, CH_3-CO complex, ICO, I_2, and C_2H_6. Intense lines of CH_3 and weak lines of C_2H_6 were readily identified upon photolysis of the CH_3I/CO/*p*-H_2 matrix sample. In experiments with $CH_3C(O)Cl$/*p*-H_2 matrices, CH_3CO was identified with a characteristic intense line at 1880.5 cm^{-1} and four moderately intense lines at 2989.1, 1419.9, 1323.2, and 836.6 cm^{-1}, as discussed in Sec. V A. The intensities of observed new lines in group Y increased significantly upon annealing of the UV-irradiated matrix of CH_3I/CO/*p*-H_2; these lines do not correspond to those of CH_3, C_2H_6, or CH_3CO.

Among the observed lines in group Y, two weak features at 3164.5/3165.7 and 1396.4/1397.6 cm^{-1} and an intense line at 613.0 cm^{-1} have vibrational wavenumbers only slightly smaller than those observed for CH_3 at 3170.6/3171.6, 1401.7/1402.7/1402.4, and 624.3/623.1 cm^{-1},[42] indicating the presence of a perturbed CH_3 moiety. The intense line observed at 2150.1 cm^{-1} in group Y has a vibrational wavenumber slightly greater than those of CO observed in the range of 2138−2146 cm^{-1} in solid *p*-H_2, indicating a perturbed moiety of CO. These lines in group Y, enhanced upon annealing of the UV-irradiated CH_3I/CO/*p*-H_2 matrix, are hence likely due to a CH_3-CO complex produced from the reaction CH_3 + CO. Lines of the CH_3 moiety were observed to be redshifted from those of isolated CH_3 by ∼6, 5, and 11 cm^{-1} for lines at 3164.5/3165.7, 1396.4/1397.6, and 613.0 cm^{-1}, whereas the line of the CO moiety at 2150.1 cm^{-1} was blueshifted by 9.5 cm^{-1} from the Q(0) line of CO at 2140.6 cm^{-1}.

The observed and quantum-chemically predicted vibrational wavenumbers of CH_3 and CH_3-CO are compared in Table II. Quantum-chemical calculations using the B3LYP/6-311G (2*d*,2*p*) method predicted that the two most intense IR lines of the CH_3-CO complex have anharmonic vibrational wavenumbers at 2190 and 669 cm^{-1} and four weaker ones at 3144, 3142, 1380, and 1379 cm^{-1}; our observed value deviates within 8.0% of these predicted values. Predicted redshifts of 4−5 cm^{-1} for lines near 3165 and 1397 cm^{-1} are in satisfactory agreements with experimental observations, but the line at 613 cm^{-1}, observed to have a redshift of 11.1 cm^{-1} from that of CH_3, was predicted to have a redshift of ∼30 cm^{-1}. This effect might be due to the large negative anharmonic corrections from 504 to 703 cm^{-1} for CH_3 and from 517 to 669 cm^{-1} for CH_3-CO; a more sophisticated method is needed to describe properly the potential-energy surface corresponding to this vibrational mode. Observation of a single line at 2150.1 cm^{-1} slightly blue-shifted from the rotational lines of CO is consistent with the fact that upon complex formation CO does not rotate and the C=O bond is strengthened. A similar blueshift of the CO line was observed in the complex Cl_2-CO with the carbon atom as the interacting site; in contrast, a redshift was observed for the complex CO-Cl_2 with the oxygen atom as the interacting site.[71]

D. Mechanism for photolysis of $CH_3C(O)Cl$ in solid *p*-H_2

Five primary channels are energetically accessible at 248 nm (482 kJ mol^{-1}):

$$CH_3C(O)Cl \rightarrow CH_3CO + Cl, \quad (1)$$

$$\rightarrow CH_2CO + HCl, \quad (2)$$

$$\rightarrow CH_3Cl + CO, \quad (3)$$

$$\rightarrow CH_3 + ClCO, \quad (4)$$

$$\rightarrow \bullet CH_2C(O)Cl + H. \quad (5)$$

The experimental dissociation energy of the C−Cl bond, D_0(C−Cl), is 350 kJ mol^{-1},[72] which is near the theoretical values of 349 and 345 kJ mol^{-1} calculated with the UCCSD(T)/CBS//UCCSD(T)/aug-cc-pVTZ[27] and the G4//B3LYP/6-311++G(3df,2p) methods.[73] Experimental enthalpies of reaction at 298 K for channels (2)−(4) were reported to be 103, 50, and 367 kJ mol^{-1}.[60] According to CCSD(T)/cc-pVTZ//B3LYP/6-311G (d,p) calculations, channels (2) and (3) involve reaction barriers of heights 190−309 and 364 kJ mol^{-1}, respectively.[29] ΔH^o_f of $\bullet CH_2C(O)Cl$ at 0 K was reported to be −26 kJ mol^{-1} and the C−H bond energy in $CH_3C(O)Cl$ is ∼422 kJ mol^{-1},[74] consistent with the value of 402 kJ mol^{-1} predicted with the

CCSD(T)/cc-pVTZ//B3LYP/6-311G(d,p) method.[29] According to molecular-beam experiments, upon irradiation of $CH_3C(O)Cl$ at 248 or 235 nm, the primary dissociation channel is the C−Cl bond fission;[20,27] about 30% of the CH_3CO product dissociates further to $CH_3 + CO$.[24,25] Because energy quenching is expected to be facile in solid *p*-H_2, likely a greater fraction of CH_3CO radicals is stabilized in our experiment.

The mixing ratios of $CH_3C(O)Cl$ and photolysis products CH_3CO, CH_2CO, HCl, CH_3, and CO as a function of photolysis period, presented in Fig. 3, indicates that the fission of the C−Cl bond leading to the formation of stabilized CH_3CO and Cl (reaction (1)) is the primary channel. The spin-orbit transition of Cl at 943.7 cm^{-1} was unobservable because of its small absorption cross section of 9.5×10^{-26} km $molecule^{-1}$.[75] The growth patterns of HCl and CH_2CO are similar to that of CH_3CO, indicating that they might be produced directly upon photo-irradiation, but the possibility of formation due to secondary photolysis or reaction could not be definitively excluded because of the nature of our experiments using continuous radiation for photolysis. We identified no CH_3Cl;[58] because CH_3Cl cannot be photolyzed at 248 nm, this result indicates the absence of reaction (3). The product ClCO in reaction (4) was reported to absorb at 1880.4 cm^{-1} in solid *p*-H_2 (Ref. 40) and at 1884.6 cm^{-1} in the gaseous phase,[69] but the absorption of CH_3CO at 1880.5 cm^{-1} interfered with this observation. No absorption line of $•CH_2C(O)Cl$, predicted to have characteristic lines near 1682, 1136, and 602 cm^{-1}, was identified.

The formation of CH_3CO increased more rapidly initially, but the increase became slower subsequently. Considering that the initial concentration of $CH_3C(O)Cl$ was 210 ± 40 ppm, and that the decay was only ∼14 ppm after irradiation for 2 h, CH_3CO likely underwent secondary photodissociation or recombination with Cl to yield $CH_3C(O)Cl$ and other products. This condition is rationalized by its UV absorption cross section of $\sim 1 \times 10^{-18}$ cm^2 $molecule^{-1}$ at 248 nm.[5] The intensities of lines of products HCl and CH_2CO also increased with behavior similar to those lines of CH_3CO, but the small intensities defy a definitive confirmation of such behavior.

To have an acceptable S/N ratio and to minimize secondary processes as much as possible, we chose an irradiation period of 30 min to estimate the mixing ratios of CH_3CO, CH_2CO, CO, and CH_3 as approximately (4.5 ± 0.6), (1.15 ± 0.1), (0.20 ± 0.03), and (0.5 ± 0.1) ppm, respectively; the corresponding branching ratios of (0.71 ± 0.09), (0.18 ± 0.01), (0.03 ± 0.01), and (0.08 ± 0.02) were estimated. The error limits reflect only one standard deviation among results obtained from several lines of each species. The systematic error might be as large as twice the estimated values for CH_3CO and CH_3 because theoretically predicted IR intensities were used and we assumed that all products were primary photofragments. Because of the limitations posed by the nature of our experiments, the branching ratio for channel (2), 0.7 ± 0.1, should be taken as a lower limit because some CH_3CO might dissociate upon irradiation or reacts further with Cl or other species. The estimated yield for formation of CH_2CO and HCl, 18%, should be taken as an upper limit for reaction (2) because of possible secondary reaction to form CH_2CO. The most significant result is that CH_3CO is the major product upon irradiation of the $CH_3C(O)Cl/p$-H_2 matrix, in contrast to the observation of only the HCl-CH_2CO complex when $CH_3C(O)Cl$ isolated in an Ar-matrix was irradiated with light at 248 nm.[16] Our observation of CH_3CO rather than the HCl-CH_2CO complex as a major product demonstrates again the advantage of a diminished cage effect of *p*-H_2 to produce free radicals *via* photolysis *in situ*.

E. Mechanism for formation of the CH_3-CO complex

The purpose of the $CH_3I/CO/p$-H_2 photolysis experiments was to investigate the products of the reaction of $CH_3 + CO$. In the gaseous phase, photolysis of CH_3I at 254 nm produces CH_3 with translational energy of ∼134 kJ mol^{-1}.[76] This translational energy of CH_3 corresponds to ∼87 kJ mol^{-1} in the center-of-mass coordinates of the $CH_3 + CO$ system, greater than the barrier of 25−27 kJ mol^{-1} for the formation of CH_3CO.[7,33,34] The internal energy of CH_3 was also estimated to be 42 kJ mol^{-1}.[76] The observation of only CH_3-CO, not CH_3CO, upon UV irradiation of the $CH_3I/CO/p$-H_2 matrix indicates that the excess energy of CH_3 upon photolysis of CH_3I was readily quenched in solid *p*-H_2 so that the barrier for formation of CH_3CO was not overcome. The kinetic energy of the $CH_3 + CO$ system was near zero upon annealing so that the barrier could not be overcome either. The formation of the CH_3-CO complex is barrierless so that the reaction of $CH_3 + CO \rightarrow CH_3$-CO is feasible upon annealing of the UV-irradiated matrix. Bennett *et al.* irradiated CH_4/CO in ice at 10 K with electrons at 5 keV to generate CH_3 radical for the reaction $CH_3 + CO$ and also failed to observe the formation of CH_3CO.[34]

We have performed several bimolecular reactions in solid *p*-H_2 to produce free radicals.[35] Most reactions are barrierless, for example: $Cl + CS_2 \rightarrow ClSCS$,[77] $CH_3 + SO_2 \rightarrow CH_3SO_2$,[42] and reactions of Cl with $CH_3CH{=}CH_2$, t-butadiene, C_6H_6, and C_5H_5N to form $•CH_2CHClCH_3$,[78] $•(CH_2CHCH)CH_2Cl$,[79] σ-complex ClC_6H_6,[80] and C_5H_5N-Cl,[80] respectively. A small barrier ∼2 kJ mol^{-1} was predicted for the reaction of Cl with C_2H_4 and C_2H_2, and reaction products CH_2CH_2Cl (Ref. 81) and $C_2H_3Cl + CHClCH_3$ were observed.[82] Apparently, the barrier height of ∼27 kJ mol^{-1} was too large for reactions to occur in solid *p*-H_2. This condition indicates a limitation to the application of photo-induced bimolecular reactions to produce free radicals in solid *p*-H_2 such that only reactions with negligible barriers can occur within these low-temperature solid *p*-H_2 environments.

VI. CONCLUSION

Irradiation at 248 nm of a $CH_3C(O)Cl/p$-H_2 matrix at 3.2 K produced new features at 2990.3, 2989.1, 2915.6, 1880.5, 1419.9, 1323.2, 836.6, and possibly 468.1 cm^{-1} that are assigned to the CH_3CO radical; we extended previous observation of only three most intense lines to eight lines. When a matrix of $CD_3C(O)Cl/p$-H_2 was used, lines at 2246.2, 2244.0, 1866.1, 1046.7, 1029.6, 1027.5, 889.1, and

723.8 cm^{-1} were observed and assigned to CD_3CO; all lines except that at 1866.1 cm^{-1} are newly observed. When a matrix of $CH_3I/CO/p\text{-}H_2$ at 3.2 K was irradiated at 248 nm and, subsequently, annealed at 5.1 K, new lines at 3165.7, 3164.5, 2150.1, 1397.6, 1396.4, and 613.0 cm^{-1} were observed and assigned to the CH_3-CO complex. All spectral assignments are based on their photochemical behavior, available D-isotopic shifts, and comparison of observed wavenumbers and intensities with calculations.

The observation of CH_3CO radical as the major product from photolysis of $CH_3C(O)Cl$ serves as an additional example to illustrate that solid $p\text{-}H_2$ has a diminished cage effect such that isolated CH_3CO radicals and Cl atoms were produced upon UV photolysis of $CH_3C(O)Cl$, in contrast to experiments in the Ar matrix in which only CH_2CO and HCl were observed. Similarly, the formation of CH_3 radical from CH_3I and its subsequent reaction with CO to form a CH_3-CO complex also demonstrate the diminished cage effect of solid $p\text{-}H_2$. Observation of a CH_3-CO complex but not the CH_3CO radical upon photolysis of a $CH_3I/CO/p\text{-}H_2$ matrix indicates that the kinetic energy of CH_3 upon photolysis of CH_3I was readily quenched so that the barrier height of $\sim$27 kJ mol^{-1} for the reaction of $CH_3 + CO$ could not be overcome. This result indicates that the application of photo-induced bimolecular reactions to prepare free radicals in solid $p\text{-}H_2$ is limited to reactions with negligible barrier.

ACKNOWLEDGMENTS

Ministry of Science and Technology, Taiwan (Grant No. NSC102-2745-M009-001-ASP) and Ministry of Education, Taiwan ("Aim for the Top University Plan" of National Chiao Tung University) supported this work. The National Center for High-Performance Computation provided computer time.

[1]B. J. Finlayson-Pitts and J. N. Pitts, Jr., *Atmospheric Chemistry: Fundamentals and Experimental Techniques* (Wiley, New York, 1986).
[2]L. K. Huynh and A. Violi, J. Org. Chem. **73**, 94 (2008).
[3]G. D. Castro, M. H. Costantini, and J. A. Castro, Hum. Exp. Toxicol. **28**, 203 (2009).
[4]J. V. Michael, D. G. Keil, and R. B. Klemm, J. Chem. Phys. **83**, 1630 (1985).
[5]M. M. Maricq and J. J. Szente, Chem. Phys. Lett. **253**, 333 (1996).
[6]B. Rajakumar, J. E. Flad, T. Gierczak, A. R. Ravishankara, and J. B. Burkholder, J. Phys. Chem. A **111**, 8950 (2007).
[7]K. W. Watkins and W. W. Word, Int. J. Chem. Kinet. **6**, 855 (1974).
[8]D. A. Parkes, Chem. Phys. Lett. **77**, 527 (1981).
[9]B. Klotz, F. Graedler, S. Sorensen, I. Branes, and K.-H. Becker, Int. J. Chem. Kinet. **33**, 9 (2001).
[10]B. Rajakumar, T. Gierczak, J. E. Flad, A. R. Ravishankara, and J. B. Burkholder, J. Photochem. Photobiol. A **199**, 336 (2008).
[11]J. E. Bennett and B. Mile, Trans. Faraday Soc. **67**, 1587 (1971).
[12]J. S. Shirk and G. C. Pimental, J. Am. Chem. Soc. **90**, 3349 (1968).
[13]M. E. Jacox, Chem. Phys. **69**, 407 (1982).
[14]M. G. K. Thompson, M. R. White, B. D. Linford, K. A. King, M. M. Robinson, and J. M. Parnis, J. Mass Spectrom. **46**, 1071 (2011).
[15]B. Rowland and W. P. Hess, Chem. Phys. Lett. **263**, 574 (1996).
[16]B. Rowland, P. R. Winter, G. B. Ellison, J. G. Radziszewski, and W. P. Hess, J. Phys. Chem. A **103**, 965 (1999).
[17]N. Kogure, T. Ono, E. Suzuki, and F. Watari, J. Mol. Struct. **296**, 1 (1993).
[18]B. Rowland and W. P. Hess, J. Phys. Chem. A **101**, 8049 (1997).
[19]E. Arunan, J. Phys. Chem. A **101**, 4838 (1997).
[20]M. D. Person, P. W. Kash, and L. J. Butler, J. Chem. Phys. **97**, 355 (1992).
[21]M. D. Person, P. W. Kash, and L. J. Butler, J. Phys. Chem. **96**, 2021 (1992).
[22]S. Deshmuk, J. D. Myers, S. S. Xantheas, and W. P. Hess, J. Phys. Chem. **98**, 12535 (1994).
[23]T. Shibata and T. Suzuki, Chem. Phys. Lett. **262**, 115 (1996).
[24]S. North, D. A. Blank, and Y. T. Lee, Chem. Phys. Lett. **224**, 38 (1994).
[25]S. Deshmukh and W. P. Hess, J. Chem. Phys. **100**, 6429 (1994).
[26]T. Shibata, H. Li, H. Katayanagi, and T. Suzuki, J. Phys. Chem. A **102**, 3643 (1998).
[27]X. Tang, B. J. Ratliff, B. L. FitzPatrick, and L. J. Butler, J. Phys. Chem. B **112**, 16050 (2008).
[28]E. A. Fogleman, H. Koizumi, J. Kercher, B. Sztaray, and T. Baer, J. Phys. Chem. A **108**, 5288 (2004).
[29]Y. T. Liu, M. T. Tsai, C. Y. Liu, P. Y. Tsai, K. C. Lin, Y. H. Shih, and A. H. H. Chang, J. Phys. Chem. A **114**, 7275 (2010).
[30]R. Sumathi and A. K. Chandra, J. Chem. Phys. **99**, 6531 (1993).
[31]R. Sumathi and A. K. Chandra, Chem. Phys. **181**, 73 (1994).
[32]S. L. Chen and W. H. Fang, J. Phys. Chem. A **111**, 9355 (2007).
[33]C. Anastasi and P. R. Maw, J. Chem. Soc., Faraday Trans. 1 **78**, 2423 (1982).
[34]C. J. Bennett, C. S. Jamieson, Y. Osamura, and R. I. Kaiser, Astrophys. J. **624**, 1097 (2005).
[35]M. Bahou, P. Das, Y.-F. Lee, Y.-J. Wu, and Y.-P. Lee, Phys. Chem. Chem. Phys. **16**, 2200 (2014).
[36]T. Momose, M. Fushitani, and H. Hoshina, Int. Rev. Phys. Chem. **24**, 533 (2005).
[37]K. Yoshioka, P. L. Raston, and D. T. Anderson, Int. Rev. Phys. Chem. **25**, 469 (2006).
[38]M. Bahou, C.-W. Huang, Y.-L. Huang, J. Glatthaar, and Y.-P. Lee, J. Chin. Chem. Soc. **57**, 771 (2010).
[39]M. E. Fajardo, *Physics and Chemistry at Low Temperatures*, edited by L. Khriachtchev (Pan Stanford Publishing Pte. Ltd., Singapore, 2011), p. 167.
[40]P. Das and Y.-P. Lee, J. Chem. Phys. **139**, 084320 (2013).
[41]Y.-F. Lee, L.-J. Kong, and Y.-P. Lee, J. Chem. Phys. **136**, 124510 (2012).
[42]Y.-F. Lee and Y.-P. Lee, J. Chem. Phys. **134**, 124314 (2011).
[43]Y.-P. Lee, Y.-J. Wu, R. M. Lees, L.-H. Xu, and J. T. Hougen, Science **311**, 365 (2006).
[44]P. L. Raston and D. T. Anderson, Phys. Chem. Chem. Phys. **8**, 3124 (2006).
[45]M. Ruzi and D. T. Anderson, J. Chem. Phys. **137**, 194313 (2012).
[46]W. S. Benedict, R. Herman, G. E. Moore, and S. Silverman, J. Chem. Phys. **26**, 1671 (1957).
[47]M. J. Frisch, G. W. Trucks, H. B. Schlegel *et al.*, GAUSSIAN 09, Revision A02, Gaussian, Inc., Wallingford, CT, 2009.
[48]A. D. Becke, J. Chem. Phys. **98**, 5648 (1993).
[49]J. P. Perdew, K. Burke, and Y. Wang, Phys. Rev. B **54**, 16533 (1996).
[50]R. Krishnan, J. S. Binkley, R. Seeger, and J. A. Pople, J. Chem. Phys. **72**, 650 (1980).
[51]A. D. McLean and G. S. Chandler, J. Chem. Phys. **72**, 5639 (1980).
[52]A. V. Kudich, V. A. Bataev, and I. A. Godunov, Russ. Chem. Bull. Int. Ed. **54**, 62 (2005).
[53]S. Tsuchiya and T. Iijima, J. Mol. Struct. **13**, 327 (1972).
[54]See supplementary material at http://dx.doi.org/10.1063/1.4883519 for comparison of experimental vibrational wavenumbers and relative IR intensities of $CH_3C(O)Cl$, $CD_3C(O)Cl$, CH_2CO, CD_2CO, $\bullet CH_2C(O)Cl$, $\bullet CD_2C(O)Cl$, CH_3Cl, and CD_3Cl with those calculated with the B3PW91/aug-cc-pVTZ method, vibrational wavenumbers and IR intensities of CH_3-CO calculated with the B3LYP/6-311g(2d,2p) and B3PW91/6-311g(2d,2p) methods, experimental results of photolysis of the $CD_3C(O)Cl//p\text{-}H_2$ matrix, and comparison of observed lines in group X_D (CD_3CO) with those simulated for CD_3CO, $\bullet CD_2C(O)Cl$, and CD_3Cl.
[55]M. R. Nimlos, J. A. Soderquist, and G. B. Ellison, J. Am. Chem. Soc. **111**, 7675 (1989).
[56]J. S. Francisco and N. J. Abersold, Chem. Phys. Lett. **187**, 354 (1991).
[57]B. Viskolcz and T. Berces, Phys. Chem. Chem. Phys. **2**, 5430 (2000).
[58]K. Kim, H. S. Kim, M. S. Kim, and H. Kim, Bull. Korean Chem. Soc. **10**, 161 (1989).
[59]J. Overend, R. A. Nyquist, J. C. Evans, and W. J. Potts, Spectrochim. Acta **17**, 1205 (1961).
[60]P. R. Winter, B. Rowland, W. P. Hess, J. G. Radziszewski, M. R. Nimlos, and G. B. Ellison, J. Phys. Chem. A **102**, 3238 (1998).
[61]W. F. Arendale and W. H. Fletcher, J. Chem. Phys. **26**, 793 (1957).
[62]D. T. Anderson, R. J. Hinde, S. Tam, and M. E. Fajardo, J. Chem. Phys. **116**, 594 (2002).
[63]P. Das, M. Bahou, and Y.-P. Lee, J. Chem. Phys. **138**, 054307 (2013).
[64]S. Tam and M. E. Fajardo, J. Low. Temp. Phys. **122**, 345 (2001).

[65]M. E. Fajardo, C. M. Lindsay, and T. Momose, J. Chem. Phys. **130**, 244508 (2009).
[66]H. Hoshina, M. Fushitani, T. Momose, and T. Shida, J. Chem. Phys. **120**, 3706 (2004).
[67]A. Snelson, J. Phys. Chem. **74**, 537 (1970).
[68]M. E. Jacox, J. Mol. Spectrosc. **66**, 272 (1977).
[69]S.-H. Chen, L.-K. Chu, Y.-J. Chen, I.-C. Chen, and Y.-P. Lee, Chem. Phys. Lett. **333**, 365 (2001).
[70]A. Fahr, A. K. Nayak, and M. J. Kurylo, Chem. Phys. **197**, 195 (1995).
[71]A. Schriver, L. S. Mazzuoli, P. Chaquin, and M. Bahou, J. Phys. Chem. A **103**, 2624 (1999).
[72]B. Ruscic, Active Thermochemical Tables (ATcT) ver. 1.37 and the Core (Argonne) Thermochemical Network ver.1.072 (July 2008).
[73]C. C. Womack, W.-H. Fang, D. B. Straus, and L. J. Butler, J. Phys. Chem. A **114**, 13005 (2010).
[74]A. Srivatsava, E. Arunan, G. Manke II, D. W. Setser, and R. Sumathi, J. Phys. Chem. A **102**, 6412 (1998).
[75]P. L. Raston and D. T. Anderson, J. Chem. Phys. **126**, 021106 (2007).
[76]C. D. Bass and G. C. Pimentel, J. Am. Chem. Soc. **83**, 3754 (1961).
[77]C.-W. Huang, Y.-C. Lee, and Y.-P. Lee, J. Chem. Phys. **132**, 164303 (2010).
[78]J. C. Amicangelo and Y.-P. Lee, J. Phys. Chem. Lett. **1**, 2956 (2010).
[79]M. Bahou, J.-Y. Wu, K. Tanaka, and Y.-P. Lee, J. Chem. Phys. **137**, 084310 (2012).
[80]M. Bahou, H. Witek, and Y.-P. Lee, J. Chem. Phys. **138**, 074310 (2013).
[81]J. C. Amicangelo, B. Golec, M. Bahou, and Y.-P. Lee, Phys. Chem. Chem. Phys. **14**, 1014 (2012).
[82]B. Golec and Y.-P. Lee, J. Chem. Phys. **135**, 174302 (2011).